WATER RESOURCES RESEARCH, VOL. 35, NO. 4, PAGES 943–952, APRIL 1999

Pumping tests in heterogeneous aquifers: An analytical study of what can be obtained from their interpretation using Jacob's method

Xavier Sánchez-Vila, Peter M. Meier, and Jesús Carrera

Departament Enginyeria del Terreny i Cartogràfica, Universitat Politècnica de Catalunya, Barcelona, Spain

Abstract. Interpretation of pumping tests to estimate hydraulic parameter values is typically based on the assumption of aquifer homogeneity. The applicability of the traditional methods of interpretation in real aquifers can be questioned, since the evaluation of the drawdown curves observed at different locations in a single test may not result in one consistent set of hydraulic parameters. Thus most hydrogeologists tend to look at estimated transmissivities (T) as some average property of the medium, while estimated storativities (S) are disregarded in some cases, particularly when they are obtained from data measured at the pumping well. An analytical study of drawdown under radially convergent flow toward a single point in heterogeneous aquifers shows that large time drawdown values form a straight line on a drawdown versus log time plot. Jacob's method consists of obtaining estimates for T and S from the slope and intercept of this line. We find that even in a heterogeneous field, these estimates provide valuable information about the aquifer. Estimated T values for different observation points tend to converge to a single value, which corresponds to the effective T derived under parallel flow conditions. Estimated storativities, however, display higher variability, but the geometric mean of the S_{est} values can be used as an unbiased estimator of the actual S. Thus it appears that although Jacob's method was originally derived for homogeneous media, it can provide valuable information in real aquifers.

1. Introduction

The analysis of constant-rate pumping tests is often carried out using Jacob's method [*Cooper and Jacob*, 1946]. It consists of plotting drawdown versus log time and fitting a straight line to late time data points. Estimates of the transmissivity (T) and storage coefficient (S) are obtained from the slope and intercept of this line. It is generally accepted that the estimated values (T_{est} and S_{est}) derived from Jacob's method are representative values for the test area (some area surrounding the pumping and observation wells). In fact, T_{est} values calculated from a single pumping test using drawdowns measured at different observation wells tend to be fairly constant. However, the corresponding S_{est} values display large variability. This seems to somewhat contradict the generally accepted belief that aquifer transmissivity is highly variable. Actually, *Meier et al.* [1998] and others have shown that these effects in T_{est} and S_{est} are a consequence of the homogeneity assumption used in the interpretation. Thus, in pumping tests performed in heterogeneous media, the variability in the transmissivity field is apparent as a variability in the S estimates, while the estimated T values remain almost constant. In this paper we follow up the numerical work of *Meier et al.* [1998] with an analytical study.

2. Relationship to Previous Work

Most field methods to obtain hydraulic parameter values are based on radial flow toward a well. Yet radial flow in heterogeneous media has seldom been addressed in the literature. One group of authors has studied the problem in statistical terms by defining apparent effective conductivity values as the ratio between the expected values of total flow and head gradient at a certain location. Effective transmissivity as a function of radial distance to the well in a two-dimensional domain and steady state flow is studied using either perturbation solutions [*Shvidler*, 1964; *Matheron*, 1967; *Sánchez-Vila*, 1997] or numerical methods [*Neuman and Orr*, 1993]. *Naff* [1991] and *Indelman et al.* [1996] derive effective hydraulic conductivity values for flow to a single line in three-dimensional domains. A more general work is the one by *Indelman and Abramovich* [1994b], which can be applied to infinite two- and three-dimensional domains and any type of point source terms.

A second group of authors addresses the problem of equivalent (block) parameters under steady state radial flow conditions. *Gómez-Hernández and Gorelick* [1989] use a power-averaging (empirical) approach to assign block T values in a complex groundwater flow system which includes several wells. *Desbarats* [1992] considers upscaling in a combined empirical-analytical approach. *Durlofsky* [1992] looks at different upscaling techniques to assign block T values. *Sánchez-Vila et al.* [1997] provide an analytical upscaling formula. *Tiederman et al.* [1995] consider a domain composed of two bounded regions of different T values separated by a sharp elliptical discontinuity.

All of the above authors have worked under steady state conditions. While their work provides interesting insights, pumping tests are normally performed under transient flow conditions. Here we can separate two groups of authors. In the first group the pattern of heterogeneity is well defined by the authors. *Butler* [1988] simulates pumping tests in a simple het-

Paper number 1999WR900007.
0043-1397/99/1999WR900007$09.00

erogeneous configuration consisting of a well located at the center of a circular disk embedded in a matrix of different T and S values. *Butler and Liu* [1993] place a disk of anomalous properties outside of the well. *Hunt* [1985] analyzes flow toward a well in a domain composed of n-horizontal layers, each with different properties.

Our work is most related to the second group of authors, which does not predefine the pattern for the T field but considers either real fields or that the transmissivity fields are stochastic realizations of some random space function. *Schad and Teutsch* [1994] are concerned with the estimation of the effective length scale of the heterogeneity structure based on pumping test data analysis in a real field. *Butler* [1991] studies the impact of azimuthal variations in the transmissive properties obtained from conventional pumping test analysis but in statistical terms (multiple realizations). *Lachassagne et al.* [1989] consider the relationship between the transmissivity values derived from short- and long-term pumping tests in a single aquifer, with the important conclusion that the variability of the estimates is smaller in the second case. *Oliver* [1990, 1993] is concerned with how drawdown is affected by heterogeneity; he finds that drawdown depends on a weighted average of the transmissivities in a zone of influence, which corresponds to an ellipse that encloses both the pumping and observation wells. He notices that the observation well drawdown is relatively sensitive to near-well transmissivity variation. Finally, *Serrano* [1997] derives an analytical solution for the statistics of the drawdown as a function of the statistics of transmissivity using the decomposition method.

In this framework the main objective of this paper is to assess the validity of Jacob's method in real media. Jacob's method is widely used in hydrogeology to estimate hydraulic parameters; it is therefore important for the hydrogeological community to know exactly what information is obtained when performing and analyzing a pumping test at a real site. In this work we find that the T_{est} value obtained using Jacob's method is equal to the effective transmissivity that would be derived under parallel flow conditions, and thus it is a truly representative value. However, S_{est} values contain some information about the degree of heterogeneity and therefore cannot be considered representative values by themselves (but we will see that they can be used in statistical terms to infer some properties of the aquifer).

The analysis presented here has some limitations. First, S is considered constant throughout the aquifer, based on the fact that its variability is much less significant than that of transmissivity (see, for example, *Dagan* [1989, p. 163] for a discussion on this topic); in any case, introducing a small variability in S in our analytical study would not change the most significant conclusions of the work.

The second limitation is that the analysis is carried out using a series expansion and truncating after the third term; this approach, similar to a classical perturbation expansion in a stochastic framework, has been found to work quite well in several problems related to flow in heterogeneous media, at least for mildly heterogeneous aquifers (the variance of log-T less than one). An important point to note is that since we consider a single heterogeneous field and do not pose the problem in a stochastic framework (so that T is a space function but not a random space function), our analysis is not limited by any assumption regarding the multivariate distribution of T.

3. Analytical Developments

In this section we provide an approximate analytical solution for the drawdown at any location as a function of the variations in log-T throughout the full domain. This solution is obtained using a truncated series expansion. Taking the limit of this solution for large times, we obtain the approximations to T_{est} and S_{est} that would be obtained if that particular location was used as an observation well in a pumping test and the drawdown at that well was interpreted using Jacob's method. We observe that this methodology leads to almost constant T and highly variable S estimates, as stated in the previous sections.

3.1. Expansion of the Groundwater Flow Equation

We write the groundwater flow equation in terms of drawdown, defined as the difference between the initial head value, assumed steady, and the hydraulic head at any time. If we consider the presence of a pumping well, the partial differential equation (PDE) and the boundary and initial conditions are

$$\begin{aligned} &\nabla^2 h + \nabla Y \nabla h = S \frac{\partial h}{\partial t} e^{-Y} \\ &h(\mathbf{x}, t) = 0 \qquad t = 0 \\ &\lim_{|\mathbf{x}|\to\infty} h(\mathbf{x}, t) = 0 \\ &\lim_{r\to 0} \left(r \frac{\partial h}{\partial r} \right) = \frac{Q}{2\pi T_w} \end{aligned} \tag{1}$$

where $h(\mathbf{x}, t)$ is the drawdown, $Y(\mathbf{x}) = \ln T$, Q is the (constant) total flow withdrawn at the well, and T_w is the transmissivity value at the well location. This last term can be assumed constant even in heterogeneous media, as the integral scale of Y is always much larger than the well radius.

An exact analytical solution for h cannot be found for arbitrarily variable Y. To partially overcome this problem, we expand the drawdown as $h = h^{(0)} + h^{(1)} + h^{(2)} + \cdots$. Approximations to h are obtained by truncating this expansion. Deriving the $h^{(i)}$ terms is done by expanding Y around some value. It is convenient to expand it around its mean, so that $Y = \langle Y \rangle + Y'$, where $\langle Y \rangle$ is the mean value and Y' is a space function. The next step is expanding h and Y. This way, we get an equation which involves all the $h^{(i)}$ terms:

$$\begin{aligned} &\nabla^2(h^{(0)} + h^{(1)} + h^{(2)} + \cdots) + \nabla Y' \nabla(h^{(0)} + h^{(1)} + h^{(2)} + \cdots) \\ &\quad - \frac{S}{T_G}\left(1 - Y' + \frac{1}{2}Y'^2 + \cdots\right)\frac{\partial}{\partial t} \\ &\quad \cdot (h^{(0)} + h^{(1)} + h^{(2)} + \cdots) = 0 \end{aligned} \tag{2}$$

This equation can be solved in an iterative way. There are infinite possibilities to select the iterative procedure from this equation, although not all of them are necessarily convergent. From these, the most convenient way is to write a set of equations so that equation i contains all the terms in $Y'^k h^{(j)}$, with $k + j = i$. These equations are then written as

$$L h^{(i)} = f_i(Y' h^{(0)}, Y'^{i-1} h^{(1)}, \cdots, Y' h^{(i-1)}) \tag{3}$$

where L is a linear operator. This way we can find the solution for $h^{(i)}$ sequentially (starting with $h^{(0)}$). In our case, $L = \nabla^2 - (S/T_G)(\partial/\partial t)$, and $T_G = \exp(\langle Y \rangle)$, which would

correspond to the geometric mean of the point T values if the univariate distribution of T is multi–log-Gaussian.

As we have nonhomogeneous boundary conditions, we could still have infinite possibilities for the expansion of h. For convenience, we select the $h^{(i)}$ functions so that all the nonhomogeneous boundary conditions are applied to $h^{(0)}$; then the last boundary condition in (1) becomes

$$\lim_{r\to 0}\left(r\frac{\partial h^{(0)}}{\partial r}\right)=\frac{Q}{2\pi T_w};\quad \lim_{r\to 0}\left(r\frac{\partial h^{(i)}}{\partial r}\right)=0\quad \forall\, i>0 \tag{4}$$

Again, we could use any other choice of conditions. The thing to keep in mind is that this choice will determine the closeness of our truncated solution to the true one. In any case, the truncated solution should be checked independently (e.g., numerically).

3.2. The Solution for $h^{(0)}$

The first equation in the sequential set, equation (3), is

$$\nabla^2 h^{(0)}-\frac{S}{T_G}\frac{\partial h^{(0)}}{\partial t}=0 \tag{5}$$

The solution for this equation with the initial and boundary conditions given in (2) and (4) can be obtained following the well-known steps to derive the Theis solution. This leads to

$$h^{(0)}=\frac{Q}{4\pi T_w}\int_u^\infty\frac{e^{-x}}{x}\,dx=\frac{Q}{4\pi T_w}W(u) \tag{6}$$

where $u=r^2S/4T_Gt$, and $W(u)$ (the exponential integral function in equation (6)) is called the well function in hydrogeology. Note that this first term in the expansion of h is similar to the Theis solution, except that there are two different transmissivities involved: T_w and T_G. Only in the particular case where $T_w=T_G$ does the solution correspond exactly to Theis solution in a homogeneous aquifer.

3.3. The Term $h^{(1)}$

The equation for $h^{(1)}$ is given by

$$\nabla^2 h^{(1)}-\frac{S}{T_G}\frac{\partial h^{(1)}}{\partial t}=-\nabla\cdot(Y'\nabla h^{(0)}) \tag{7}$$

By substituting (6) into (7) and applying Leibniz's rule, we get

$$\nabla^2 h^{(1)}-\frac{S}{T_G}\frac{\partial h^{(1)}}{\partial t}=\frac{Q}{2\pi T_w}\frac{1}{r}\frac{\partial}{\partial r}\left(Y'\exp\left(-\frac{r^2S}{4T_Gt}\right)\right) \tag{8}$$

with homogeneous boundary and initial conditions. The solution for (8) expressed in polar coordinates $(r,\ \theta)$ can be written in terms of fundamental solutions as

$$h^{(1)}=\frac{-Q}{2\pi T_w}\int_0^t\int_V\frac{1}{\rho}\frac{\partial}{\partial\rho}\left(Y'(\boldsymbol{\rho})\exp\left(\frac{-\rho^2S}{4T_G\tau}\right)\right)\cdot G(\mathbf{r},\boldsymbol{\rho},t,\tau)\,dV\,d\tau \tag{9}$$

where $\mathbf{r}=(r,\ \theta)$, $\boldsymbol{\rho}=(\rho,\ \phi)$, $dV=\rho d\rho d\phi$, and $G(\mathbf{r},\boldsymbol{\rho},t,\tau)$ is the fundamental solution associated to the PDE (8), which is given by

$$G(\mathbf{r},\boldsymbol{\rho},t,\tau)=\frac{1}{4\pi(t-\tau)}\exp\left(\frac{-|\mathbf{r}-\boldsymbol{\rho}|^2S}{4T_G(t-\tau)}\right) \tag{10}$$

This type of solution (Green's function) is widely used in the physical sciences [*Carslaw and Jaeger*, 1959, p. 353].

The limit of (9) for large t values is given in Appendix A:

$$h^{(1)}\to\frac{Q}{4\pi T_w}\left[\frac{-1}{\pi}\int_V Y'(\rho,\ \phi)U(r,\ \rho,\ \theta,\ \phi)\frac{1}{\rho}\,dV+(Y_w-\langle Y\rangle)\ln\frac{2.25T_Gt}{r^2S}-\overline{Y'}(R)\ln\frac{2.25T_Gt}{R^2S}\right] \tag{11}$$

where

$$U(r,\ \rho,\ \theta,\ \phi)=\frac{\rho-r\cos(\theta-\phi)}{\rho^2+r^2-2\rho r\cos(\theta-\phi)} \tag{12a}$$

$$\overline{Y'}(R)=\lim_{\rho\to\infty}\frac{1}{2\pi}\int_0^{2\pi}Y'(\rho,\ \phi)\,d\phi \tag{12b}$$

$\overline{Y'}(R)$ being the average value of Y' at infinity. By definition, $\langle Y'\rangle=0$, and therefore $\overline{Y'}(R)$ should tend to zero whenever ergodicity can be assumed, certainly for all cases of practical interest.

3.4. Analysis of the Estimated Storativity

For large t values we can now write the solution for h as approximated by $h^{(0)}+h^{(1)}$ (the first two terms in the series expansion):

$$h\simeq\frac{Q}{4\pi T_w}\left[\ln\left(\frac{2.25T_Gt}{r^2S}\right)(1+Y_w-\langle Y\rangle)-\frac{1}{\pi}\int_V Y'(\rho,\ \phi)U(r,\ \rho,\ \theta,\ \phi)\frac{1}{\rho}\,dV\right] \tag{13}$$

This could be seen as the first few terms in an exponential expansion, an argument very commonly used in hydrogeology (since *Gelhar and Axness* [1983]) but which has been recently shown to fail in certain cases [*Indelman and Abramovich*, 1994a]. The final term could be taken as

$$h\simeq\frac{Q}{4\pi T_w}\exp(Y_w-\langle Y\rangle)\cdot\left[\ln\frac{2.25T_Gt}{r^2S}-\frac{1}{\pi}\int_V Y'(\rho,\ \phi)U(r,\ \rho,\ \theta,\ \phi)\frac{1}{\rho}\,dV\right] \tag{14}$$

where we have used the idea that a term in $(Y_w-\langle Y\rangle)Y'(\rho,\ \phi)$ would appear in the next term of the series expansion. This form of the equation can only be conjectured analytically from the expansion, but can be checked numerically, as we will present later. Since $\exp(Y_w-\langle Y\rangle)=T_w/T_G$, we have finally

$$h\simeq\frac{Q}{4\pi T_G}\cdot\left[\ln t+\ln\left(\frac{2.25T_G}{r^2S}\exp\left(\frac{-1}{\pi}\int_V Y'(\rho,\ \phi)U(r,\ \rho,\ \theta,\ \phi)\frac{1}{\rho}\,dV\right)\right)\right] \tag{15}$$

This is the equation of a straight line in an h versus $\log t$ plot. Using Jacob's method, we could obtain now the first-order approximations of estimated T and S up to the second term ($h^{(1)}$) in the series expansion. The estimated T is then a constant value, equal to T_G, while the estimated S depends on the location of the observation point with respect to the pumping well. S_{est} can be obtained by direct identification with the large time equation used in Jacob's method (assuming $T_G = T_{est}$):

$$h = \frac{Q}{4\pi T_G} \ln\left(\frac{2.25 T_G t}{r^2 S_{est}}\right) \tag{16}$$

and so finally

$$S_{est}(r, \theta) = S \exp\left(\frac{1}{\pi}\int_V Y'(\rho, \phi) U(r, \rho, \theta, \phi) \frac{1}{\rho} dV\right) \tag{17}$$

Obviously, when $Y' = 0$ (homogeneous case), $S_{est} = S$; that is, it converges to the actual S value (assuming it exists and is constant). Otherwise, (17) can be viewed as a weighted average of Y' (departures of log transmissivity with respect to its mean) at any point P, where P extends throughout the full domain. The weighting function is negative in a circle whose diameter is given by the pumping and observation wells. Moreover, maximum values of these weights are achieved along this diameter. That is, if transmissivities at the points located between the pumping and observation wells are above the mean, the integral in (17) will be negative and S_{est} will be less than the true storage coefficient S, and vice versa. The points outside this area will also contribute to the integral, but their weights are smaller.

This interpretation can be rewritten by saying that whenever the observation point is connected to the pumping well by high T paths, the drawdown response will be fast. A fast response is interpreted by Jacob's method as an unduly small storativity. The reverse is true whenever transmissivities between the two points are small, as indicated by *Schad and Teutsch* [1994]. This issue will be further illustrated in section 4.

3.5. The Term $h^{(2)}$

Section 3.4 leads us to conclude that when considering only the first two terms in the series expansion, estimated transmissivity would be equal to T_G, regardless of the observation point location. In order to get improved results, we need to find an additional term in the expansion of h. The third term is the solution of the following PDE:

$$\nabla^2 h^{(2)} - \frac{S}{T_G}\frac{\partial h^{(2)}}{\partial t} = -\frac{1}{2}\nabla\cdot(Y'^2\nabla h^{(0)}) - \nabla\cdot(Y'\nabla h^{(1)}) \tag{18}$$

with homogeneous boundary conditions. Our objective is to find whether for large times the solution of (18) gives a term proportional to $\ln t$. This term will then be a higher-order correction for T_{est} at each observation well location. To get the same-order correction for S_{est}, we would need to keep also all the terms that tend to a constant for large times, but as we will see later in a numerical simulation, the result already obtained for S_{est} (equation (17)) is enough to capture most of the important effects of heterogeneity.

To solve (18), we write $h^{(2)} = h_a^{(2)} + h_b^{(2)}$, so that

$$\nabla^2 h_a^{(2)} - \frac{S}{T_G}\frac{\partial h_a^{(2)}}{\partial t} = -\frac{1}{2}\nabla\cdot(Y'^2\nabla h^{(0)}) \tag{19a}$$

$$\nabla^2 h_b^{(2)} - \frac{S}{T_G}\frac{\partial h_b^{(2)}}{\partial t} = -\nabla\cdot(Y'\nabla h^{(1)}) \tag{19b}$$

The advantage is that now the behavior of $h_a^{(2)}$ for large t values can be obtained by comparing (7) with (19a). It is clear that the same solution would hold by replacing Y' with $Y'^2/2$ in the solution (given in equation (11)), where now we need only keep the terms in $\ln t$. The final result is then

$$\lim_{t\to\infty}\frac{h_a^{(2)}}{\ln t} = \frac{Q}{4\pi T_w}\left[\frac{(Y_w - \langle Y\rangle)^2}{2} - \frac{\overline{Y'^2}(R)}{2}\right] \tag{20}$$

where $\overline{Y'^2}(R)$ tends to σ_Y^2, although it is unimportant because this term will later cancel out. As for the solution of (19b), we start by expanding the right-hand side of the equation

$$-\nabla\cdot(Y'\nabla h^{(1)}) = \nabla_r\cdot\left(\int_0^t\int_V \frac{Q}{2\pi T_w} Y'(\mathbf{r})\frac{\partial}{\partial\rho}\cdot\left(Y'(\rho)\exp\left(\frac{-\rho^2 S}{4T_G\tau}\right)\right)\nabla_r G(\mathbf{r}, \rho, t, \tau)\frac{1}{\rho} dV\, d\tau\right) \tag{21}$$

and applying again the theory of Green's functions, the solution for $h_b^{(2)}$ becomes

$$h_b^{(2)} = \int_0^t\int_V\left[-\nabla_\rho\cdot\left(\int_0^\tau\int_{V'}\frac{Q}{2\pi T_w} Y'(\rho)\frac{\partial}{\partial\rho'}\cdot\left(Y'(\rho')\exp\left(\frac{-\rho'^2 S}{4T_G\tau'}\right)\right)\nabla_\rho G(\rho, \rho', \tau, \tau')\frac{1}{\rho'} dV'\, d\tau'\right)\right]\cdot G(\mathbf{r}, \rho, t, \tau)\, dV\, d\tau \tag{22}$$

Here we use the subscript ρ under the "del" sign to indicate that the derivatives are taken with respect to (ρ, ϕ). For large t values, the expression for $h_b^{(2)}$ is calculated in Appendix B. Finally, from (20), (B12), and (B15), we get

$$\lim_{t\to\infty}\frac{h^{(2)}}{\ln t} = \frac{Q}{4\pi T_w}\cdot\left[\frac{(Y_w - \langle Y\rangle)^2}{2} - \frac{1}{4\pi^2}\lim_{\rho\to\infty}\rho\int_0^{2\pi}\int_0^{2\pi}\int_0^{\rho} Y'(\rho, \phi)Y'(\rho', \phi')\cdot\frac{\partial}{\partial\rho'}U(\rho', \rho, \phi', \phi)\, d\rho'\, d\phi\, d\phi'\right] \tag{23}$$

3.6. Analysis of Estimated Transmissivity up to $h^{(2)}$ Order

The solution for h is approximated by $h^{(0)} + h^{(1)} + h^{(2)}$:

$$\lim_{t\to\infty}\frac{h^{(0)} + h^{(1)} + h^{(2)}}{\ln t} = \frac{Q}{4\pi T_w}\left[1 + Y_w - \langle Y\rangle + \frac{(Y_w - \langle Y\rangle)^2}{2} - \frac{1}{4\pi^2}\lim_{\rho\to\infty}\rho\int_0^{2\pi}\int_0^{2\pi}\int_0^{\rho} Y'(\rho, \phi)Y'(\rho', \phi')\cdot\frac{\partial}{\partial\rho'}U(\rho', \rho, \phi', \phi)\, d\rho'\, d\phi\, d\phi'\right] \tag{24}$$

Transmissivity estimated by Jacob's method equals the inverse of this limit (Jacob's slope) divided by $Q/4\pi$. Assuming that

the terms in brackets in (24) can be taken as the first terms in the development of an exponential, and developing the derivative of U, we get finally that from the three first terms in the series expansion, an approximation of the estimated T would be obtained as

$$T_{\text{est}} = T_G \exp\left(\frac{1}{4\pi}\lim_{\rho\to\infty}\frac{1}{\pi\rho^2}\int_0^{2\pi}\int_0^{2\pi}\int_0^{\rho} Y'(\boldsymbol{\rho})Y'(\boldsymbol{\rho}') \cdot \frac{(\rho^2+\rho'^2)\cos\Delta\phi - 2\rho\rho'}{(\rho^2+\rho'^2-2\rho\rho'\cos\Delta\phi)^2}\frac{\rho^3}{\rho'}\,dV'\,d\phi\right) \quad (25)$$

The interpretation of this integral is not as simple as that of S_{est}. However, a first conclusion is immediate by simple inspection: T_{est} does not depend on either r or θ. That is, estimated transmissivity is independent of the observation point location! Regarding the actual value of the integral, it can be viewed as a weighted average of the products of log-T departures from its mean at two points, one moving over a circumference of radius ρ and the other over the inner circle. The weighting function becomes singular when the two points get close.

In the particular case of Y being totally random or multi-Gaussian with a finite integral scale, the term inside the exponential cancels out, as the ratio between the volume where correlation is different from zero and the total volume tends to zero as ρ increases. Then, $T_{\text{est}} = T_G$. However, in general, this need not be the case, and we could obtain estimated T values different from T_G. Here we should note that *Meier et al.* [1998] showed numerically that in a non–multi-Gaussian field T_{est} was very close to the effective T that could be derived under parallel flow conditions. This effective value in a two-dimensional domain is equal to the geometric mean of the point T values only under certain restrictions. These restrictions are not necessarily satisfied in a non–multi-Gaussian field, thus leading to $T_{\text{ef}} \neq T_G$ [*Sánchez-Vila et al.*, 1996].

4. Numerical Simulation

To check the analytical solutions for S_{est} and T_{est}, given by (17) and (25), respectively, we present a numerical simulation of a pumping test in a heterogeneous aquifer. The methodology (similar to *Meier et al.* [1998]) comprises the following steps: (1) generating a heterogeneous T-field, (2) solving the transient flow equation in a two-dimensional field under a constant pumping rate using a finite element code, (3) analyzing the simulated drawdown curves for a large number of observation points by fitting a straight line to the late time data, and (4) producing maps of the T and S estimates.

The first step is the generation of the heterogeneous T-field. In our example we consider Y a multi-Gaussian field, characterized by its mean $\langle Y\rangle = 0$, variance, $\sigma_Y^2 = 1$, and isotropic correlation structure, with a spherical variogram model and an integral scale of 10 units length. The size of the simulated field is 500 × 500 units length. Simulation was performed using the code GCOSIM3D [*Gómez-Hernández and Journel*, 1993], which can generate realizations of a multi-Gaussian conductivity field using the sequential simulation algorithm.

To minimize boundary effects, the heterogeneous domain is extended by rectangular elements of increasing size, with a value of $T = T_G$. The final domain consists of a total of 291,600 elements. The finite element code FAITH [*Sánchez-Vila et al.*, 1993], designed to work in a rectangular domain, is used to simulate the pumping test and to provide the drawdown versus log-t at all nodes in the mesh. A homogeneous input storativity of 1.0 is used in the simulation. The T and S values are estimated at each node by fitting a straight line through the last three drawdown data and calculating the slope and the intercept.

The methodology is strictly valid if the influence of the homogeneous transmissivity zone surrounding the heterogeneous domain can be neglected. For this reason, simulations must be terminated before this influence starts but after the straight line has been developed. We have found from preliminary runs in our case that when we stopped the simulation after 20,000 time units, these two conditions are valid in a squared domain of size 100 × 100 elements centered at the well.

The heterogeneous 500 × 500 element domain, as well as the 100 × 100 element in which estimated values are computed, can be seen in Figure 1. Note that in the small domain, T values span over 2.5 orders of magnitude. Figure 2 shows the spatial distribution of the T estimates within the 100 × 100 domain. Figure 3 shows similar maps of the numerical (Figure 3a) and analytical (Figure 3b) S_{est} values (analytical results obtained from equation (17)) for the heterogeneous domain of Figure 1.

The following can be concluded from Figures 2 and 3: (1) T values obtained from interpreting the drawdown curves using Jacob's method are almost constant; that is, the slopes in the h versus log-t curves are very similar for all observation points; deviations around the mean are less than 4%; and the radial trend observed in the figures is a numerical artifact, since the straight line takes longer to totally develop for the points located farther away from the well. (2) The almost constant T_{est} value, which could be defined by the mean, is very close to the geometric mean of the point T values (less than 1% difference). (3) S_{est} values vary strongly in space, despite the fact that input storativity is homogeneous. (4) Analytical values for S_{est} obtained by equation (17) agree very well with the map produced numerically, which means that the first-order solution in S_{est} is capable of capturing most of the total behavior. (5) Correlation is observed between the input heterogeneous T field (Figure 1b) and the spatial distribution of the S estimates; thus estimates below average appear in zones that are well connected to the pumping well and vice versa, as suggested by *Herweijer and Young* [1991] and *Schad and Teutsch* [1994]. Contrary to these last authors, however, we observe that the S_{est} field is smoother, meaning that the contribution to the S estimates is given not only by the T values along the connecting path, but also as an average value of all the transmissivities in the full domain.

5. Geostatistical Analysis of S_{est}

From (17) and after taking log values we get

$$\ln S_{\text{est}} = \ln S + \frac{1}{\pi}\int_V Y'(\rho,\,\phi)U(r,\,\rho,\,\theta,\,\phi)\,\frac{1}{\rho}\,dV \quad (26)$$

Now taking expected values, we have the following approximation:

$$\langle \ln S_{\text{est}}\rangle \simeq \ln S \quad (27)$$

Then, in a pumping test where we have several observation points, we could use the values estimated from Jacob's method

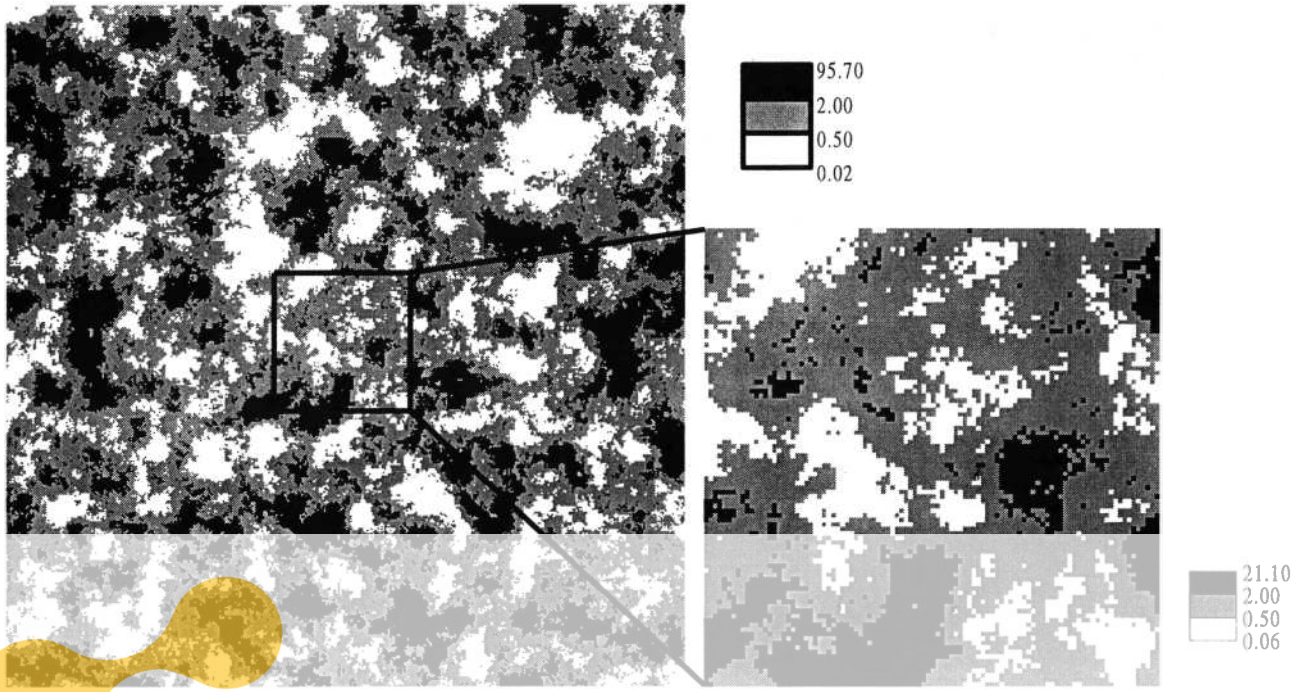

Figure 1. Heterogeneous T-field with $\langle Y \rangle = 0$ and $\sigma_Y^2 = 1.0$, of size 500 × 500, and subdomain size 100 × 100. The well is located at the center.

to get an unbiased estimator of S, which would be given by the geometric mean of the estimates:

$$S \simeq \exp\left(\frac{1}{n}\sum_{i=1}^{n} \ln S_{\text{est},i}\right) \tag{28}$$

Thus, although it is true that the S values derived from Jacob's method cannot be taken as local representative values, their geometric averages provide a good estimator of the real storativity. Unfortunately, this approach would hold only when a large number of observation wells is involved, which in field tests is seldom the case, and so a good estimator of the real storativity can rarely be obtained from pumping tests.

Since the formula used in the derivation of (27) is an approximation taking only the first two terms in the series expansion, it is important to check its validity. We use the example from the previous section to compute the mean of the ln S_{est} values with respect to distance to the pumping well. We show in Figure 4 the evolution of this mean with respect to r for both the analytical and numerical S_{est} maps given in Figure 3 (in this example, ln $S = 0$). Means are calculated by averaging the values at points which are located at a certain distance from the well. We see that for small r, the mean ln S_{est} is quite different from 0, but as the distance increases, it grows to reach values close to -0.1. The problem for small r is that there are few ln S_{est} values, so that the arithmetic mean need not be a good estimator of the expected value, but it is very much conditioned upon the particular realization we are using. For large r, however, we invoke ergodicity and may exchange the mean and the expected value. Note that even for a quite large value of the variance of log-T ($\sigma_Y^2 = 1.0$) the difference between average ln S_{est} and ln S is small (about 5–10%).

The last thing we want to analyze is the variance of the S estimates. In the numerical example we find that the sample variance is equal to 0.093 if we use the analytical estimations and is 0.085 in the numerical case. We see that in this particular example the variability in the log S estimates is about an order of magnitude smaller than the variability in log T. At this point we cannot draw any conclusion from these values. More analytical work is necessary in order to see whether there is a relationship between these two variances.

6. Summary and Conclusions

Pumping tests are the most common way to estimate hydraulic parameter values in the field. Most frequently, interpretation of these tests is carried out using Jacob's method. This method consists of fitting a straight line to the data corresponding to large times on the drawdown versus log time plot. From the slope and the intercept of this line it is possible

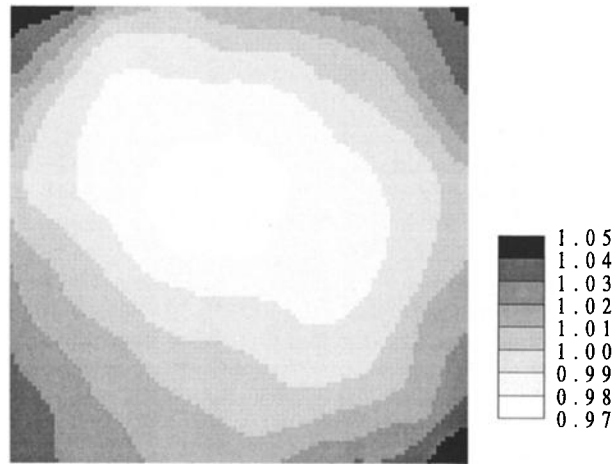

Figure 2. Spatial distribution of the numerical T estimates within the small domain in Figure 1.

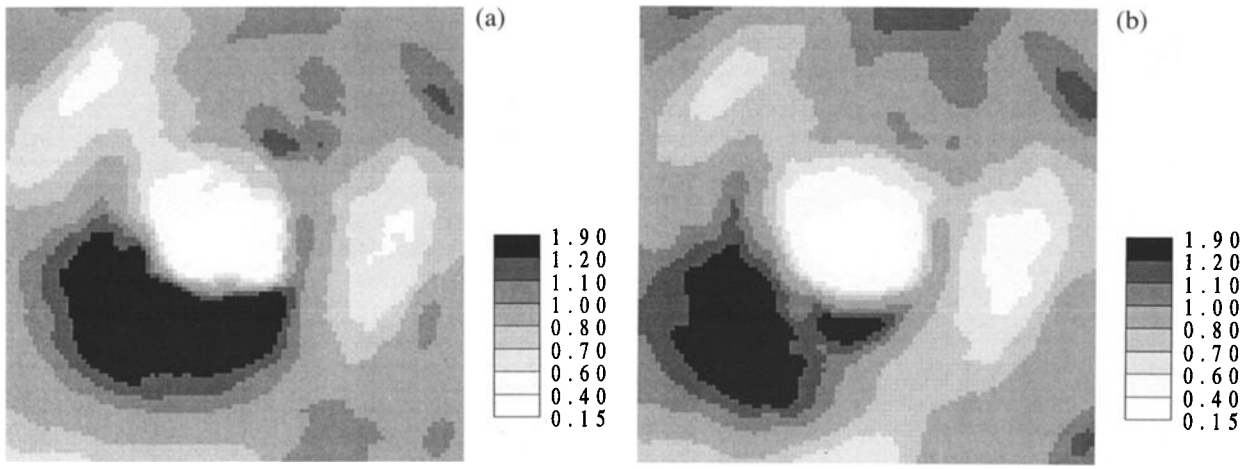

Figure 3. Spatial distribution of (a) the numerical and (b) the analytical S estimates corresponding to the small domain in Figure 1.

to obtain estimates for T and S. As is the case for most analysis methods, estimates are based on the assumption of aquifer homogeneity. Traditionally, transmissivity values estimated from this method have been looked upon as some average property of the test area, while estimated storativities are sometimes disregarded, particularly at the pumping well.

An analytical study of the large time behavior of drawdown under radially convergent flow toward a single point is presented. We consider the case of a pumping test in a real aquifer with multiple observation wells located at various directions and distances from the well. We provide an approximate analytical solution for the drawdown at any location as a function of the variations in log-T throughout the full domain. This solution is obtained using a series expansion and truncating the higher-order terms. Taking the limit of this solution for large times we obtain the approximations to T_{est} and S_{est} that would be obtained if drawdown data from an observation well were interpreted using Jacob's method. When interpreting the drawdown curves individually, we find that the T_{est} values tend to be fairly constant, while the S_{est} values display great variability.

The most important finding of this work is that the T and S estimates can provide valuable information about the aquifer. Estimated transmissivities for the different observation points tend to converge to a single value, which in a multi–log-Gaussian field corresponds to the geometric mean of the point T values. On the other hand, the geometric mean of estimated S can be used as an estimator of the real S value, assumed constant. We assess the appropriateness of the analytical expressions by a comparison with results from a numerical model.

This work sends a note of caution on the use of Jacob's method for the interpretation of long-term pumping tests for parameter estimation purposes. As is well known, the values estimated from the drawdown data are not representative values of some small support, but are rather weighted averages of the transmissivities through the full domain. This work presents this averaging function. An additional important point to make is that Jacob's method does provide much useful information: First, the estimated T value is very close to the effective T that we would obtain in the parallel flow case (e.g., equal to T_G in multi-Gaussian log-T fields). Second, estimated S values from a multiobservation well test can be used to get an estimate of the real S value (assumed constant), provided the variability of the estimates is not large (otherwise, an unrealistically large number of wells would be required). Third, these same estimates of S provide some information about the connectivity between the pumping and observation wells.

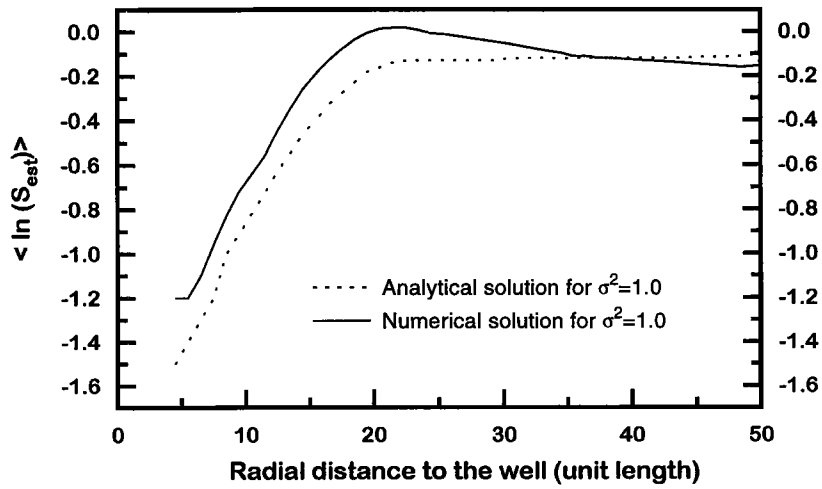

Figure 4. Evolution of the mean ln S_{est} with respect to r for the S_{est} maps in Figure 3.

Appendix A: Limit of $h^{(1)}$ for Large t Values

We start by applying parts to (9), so that

$$h^{(1)} = \frac{Q}{2\pi T_w} \cdot \left(\int_V Y'(\rho, \phi) \left[\int_0^t \exp\left(\frac{-\rho^2 S}{4T_G\tau}\right) \frac{\partial}{\partial\rho} G(\mathbf{r}, \boldsymbol{\rho}, t, \tau)\, d\tau \right] \frac{1}{\rho}\, dV - \lim_{\rho\to\infty} \int_0^{2\pi} Y'(\rho, \phi) \left[\int_0^t \exp\left(\frac{-\rho^2 S}{4T_G\tau}\right) G(\mathbf{r}, \boldsymbol{\rho}, t, \tau)\, d\tau \right] d\phi + \lim_{\rho\to 0} \int_0^{2\pi} Y'(\rho, \phi) \left[\int_0^t \exp\left(\frac{-\rho^2 S}{4T_G\tau}\right) G(\mathbf{r}, \boldsymbol{\rho}, t, \tau)\, d\tau \right] d\phi \right) \tag{A1}$$

The first thing is to integrate in τ. The way to do this is to note that the term in t is given as a convolution. It can be solved in Laplace space, knowing that the transform of the convolution is the product of transforms. Then, from the Laplace transform we can obtain the leading terms in t, which are what we are really interested in (and not in the full range of t). The integral in time corresponding to the first term in (A1) (after performing the derivative with respect to ρ) can be written as a certain functional $P(t)$, given by

$$P(t) = \int_0^t \exp\left(\frac{-b_1^2}{4\tau}\right) \frac{1}{(t-\tau)^2} \exp\left(\frac{-b_2^2}{4(t-\tau)}\right) d\tau \tag{A2}$$

where $b_1 = \rho\sqrt{S/T_G}$ and $b_2 = |\mathbf{r} - \boldsymbol{\rho}|\sqrt{S/T_G}$. Now we take the Laplace transform of this integral; from *Erdélyi et al.* [1954, p. 146] we have the following Laplace transforms:

$$L\left[\exp\left(\frac{-b_1^2}{4t}\right)\right] = \frac{b_1}{\sqrt{p}} K_1(b_1\sqrt{p}) \tag{A3}$$

$$L\left[\frac{1}{t^2}\exp\left(\frac{-b_2^2}{4t}\right)\right] = 4\frac{\sqrt{p}}{b_2} K_1(b_2\sqrt{p})$$

where $L[\ ]$ stands for Laplace transform and K_1 is the modified Bessel function of first order. Now using the convolution properties,

$$L[P(t)] = L\left[\exp\left(\frac{-b_1^2}{4t}\right)\right] L\left[\frac{1}{t^2}\exp\left(\frac{-b_2^2}{4t}\right)\right] = 4\frac{b_1}{b_2} K_1(b_1\sqrt{p}) K_1(b_2\sqrt{p}) \tag{A4}$$

Since we only want the behavior for $t \to \infty$, we can take the limit of the transform for $p \to 0$ and backtransform it

$$L[P(t)] \to \frac{4}{b_2^2}\frac{1}{p} \tag{A5}$$

which is based upon the first-order approximation of the modified Bessel function

$$\lim_{x\to 0} K_1(x) = \frac{1}{x} \tag{A6}$$

Then, finally, for large times, $P(t)$ can be taken equal to

$$\lim_{t\to\infty} P(t) = L^{-1}\left[\frac{4}{b_2^2}\frac{1}{p}\right] = 4\frac{T_G}{S}\frac{1}{|\mathbf{r}-\boldsymbol{\rho}|^2} \tag{A7}$$

We can do the same for the remaining terms in (A1). It turns out that for $t \to \infty$, the first term in (A1) becomes a constant (the one given in A7), while in the remaining two terms, the two leading terms are a function of $\ln t$ and a constant. Keeping all these terms, we can finally write that for large times

$$h^{(1)} \to \frac{Q}{4\pi T_w}\frac{1}{\pi} \cdot \int_V Y'(\rho, \phi) \left(\frac{-\rho + r\cos(\theta - \phi)}{\rho^2 + r^2 - 2\rho r\cos(\theta - \phi)} \right) \frac{1}{\rho}\, dV - \frac{Q}{4\pi T_w}\frac{1}{2\pi} \lim_{\rho\to\infty} \int_0^{2\pi} Y'(\rho, \phi)\, d\phi \left(\ln t + \ln\frac{2.25T_G}{\rho^2 S} \right) + \frac{Q}{4\pi T_w}(Y_w - \langle Y\rangle)\left(\ln t + \ln\frac{2.25T_G}{r^2 S} \right) \tag{A8}$$

which corresponds exactly to (11).

Appendix B: Limit of $h^{(2)}$ for Large t Values

We start from (22) and develop the derivatives of products, so that we get an expression which contains a sum of four terms:

$$h_b^{(2)} = -\int_0^t \int_V \left(\int_0^\tau \int_{V'} \frac{Q}{2\pi T_w} \cdot \left[\nabla_\rho Y'(\boldsymbol{\rho}) \frac{\partial}{\partial\rho'} Y'(\boldsymbol{\rho}') \nabla_\rho G - \nabla_\rho Y'(\boldsymbol{\rho}) Y'(\boldsymbol{\rho}') \frac{\rho' S}{2T_G\tau'} \nabla_\rho G + Y'(\boldsymbol{\rho}) \frac{\partial}{\partial\rho'} Y'(\boldsymbol{\rho}') \nabla_\rho^2 G - Y'(\boldsymbol{\rho}) Y'(\boldsymbol{\rho}') \frac{\rho' S}{2T_G\tau'} \nabla_\rho^2 G \right] \cdot \exp\left(\frac{-\rho'^2 S}{4T_G\tau'}\right) \frac{1}{\rho'}\, dV'\, d\tau' \right) G(\mathbf{r}, \boldsymbol{\rho}, t, \tau)\, dV\, d\tau \tag{B1}$$

and we further have that

$$\nabla_\rho^2 G = \frac{S}{T_G}\frac{\partial G}{\partial\tau} - \delta(\boldsymbol{\rho}, \boldsymbol{\rho}') \tag{B2}$$

The objective is to get the terms which give a contribution in t which is of the order $\ln t$ and to show that this is the leading contribution (no higher-order terms). All terms with lower order will be dropped. Again, the idea is to work with Laplace transforms. Although the mathematics are very involved and quite tedious, we provide a few intermediate steps of the derivation for the interested reader. First, since the bracketed term in (B1) is a sum of four terms, we decompose (B1) into a sum of four terms. The first one is

$$h_{b,\alpha}^{(2)} = \frac{-Q}{2\pi T_w} \int_0^t \int_V \int_0^\tau \int_{V'} \nabla_\rho Y'(\boldsymbol{\rho}) \frac{\partial}{\partial\rho'} Y'(\boldsymbol{\rho}') \nabla_\rho G(\boldsymbol{\rho}, \boldsymbol{\rho}', \tau, \tau') \cdot \exp\left(\frac{-\rho'^2 S}{4T_G\tau'}\right) \frac{1}{\rho'} G(\mathbf{r}, \boldsymbol{\rho}, t, \tau)\, dV'\, d\tau'\, dV\, d\tau \tag{B3}$$

Now in (B3) we isolate the part which depends on time (after writing the explicit expressions of the Green's functions), which appears as a double convolution:

$$P_1(t) = \int_0^t \int_0^\tau \exp\left(\frac{-b_1^2}{4\tau'}\right) \frac{1}{(\tau - \tau')^2} \exp\left(\frac{-b_2^2}{4(\tau - \tau')}\right) \frac{1}{(t - \tau)} \cdot \exp\left(\frac{-b_3^2}{4(t - \tau)}\right) d\tau' \, d\tau \quad \text{(B4)}$$

where $b_1 = \rho' \sqrt{S/T_G}$, $b_2 = |\boldsymbol{\rho} - \boldsymbol{\rho}'| \sqrt{S/T_G}$, and $b_3 = |\mathbf{r} - \boldsymbol{\rho}| \sqrt{S/T_G}$. Now we take the Laplace transform double convolution

$$L[P_1(t)] = 8 \frac{b_1}{b_2} K_1(b_1 \sqrt{p}) K_1(b_2 \sqrt{p}) K_0(b_3 \sqrt{p}) \quad \text{(B5)}$$

Now, following Appendix A, we take the limit of the transform for $p \to 0$ and backtransform it after keeping only the leading term. So we get

$$\lim_{t \to \infty} \frac{P_1(t)}{\ln t} = \frac{4}{b_2^2} = 4 \frac{T_G}{S} \frac{1}{|\boldsymbol{\rho} - \boldsymbol{\rho}'|^2} \quad \text{(B6)}$$

The methodology is the same for the remaining terms. The second term in (B1) is

$$h_{b,\beta}^{(2)} = \frac{Q}{2\pi T_w} \int_0^t \int_V \int_0^\tau \int_{V'} \nabla_\rho Y'(\boldsymbol{\rho}) Y'(\boldsymbol{\rho}') \frac{S}{2T_G \tau'} \nabla_\rho G(\boldsymbol{\rho}, \boldsymbol{\rho}', \tau, \tau') \cdot \exp\left(\frac{-\rho'^2 S}{4T_G \tau'}\right) G(\mathbf{r}, \boldsymbol{\rho}, t, \tau) \, dV' \, d\tau' \, dV \, d\tau \quad \text{(B7)}$$

The part which depends with time in (B7) is given as

$$P_2(t) = \int_0^t \int_0^\tau \frac{1}{\tau'} \exp\left(\frac{-b_1^2}{4\tau'}\right) \frac{1}{(\tau - \tau')^2} \exp\left(\frac{-b_2^2}{4(\tau - \tau')}\right) \cdot \frac{1}{(t - \tau)} \exp\left(\frac{-b_3^2}{4(t - \tau)}\right) d\tau' \, d\tau \quad \text{(B8)}$$

and with the same methodology we get

$$\lim_{t \to \infty} \frac{P_2(t)}{\ln t} = 0 \quad \text{(B9)}$$

Before we proceed with the remaining two terms in (B1), we substitute the expression for $P_1(t)$ into (B1) (P_2 is not necessary since it is equal to zero). So we have

$$\lim_{t \to \infty} \frac{h_{b,\alpha}^{(2)}}{\ln t} = \frac{Q}{4\pi T_w} \frac{1}{8\pi^2} \cdot \int_V \int_V \nabla_\rho Y'(\boldsymbol{\rho}) \frac{\partial}{\partial \rho'} Y'(\boldsymbol{\rho}') \frac{1}{\rho'} \nabla_\rho (\ln |\boldsymbol{\rho} - \boldsymbol{\rho}'|^2) \, dV' \, dV \quad \text{(B10)}$$

By applying the divergence theorem, we get

$$\lim_{t \to \infty} \frac{h_{b,\alpha}^{(2)}}{\ln t} = \frac{Q}{4\pi T_w} \frac{1}{4\pi^2} \cdot \left(\lim_{\rho \to \infty} \int_0^{2\pi} \rho \int_V Y'(\boldsymbol{\rho}) \frac{\partial}{\partial \rho'} Y'(\boldsymbol{\rho}') \frac{1}{\rho'} \cdot \left[\frac{\rho - \rho' \cos \Delta\phi}{\rho^2 + \rho'^2 - 2\rho\rho' \cos \Delta\phi} \right] dV' \, d\phi - \lim_{\varepsilon \to 0} \int_0^{2\pi} \varepsilon \int_V Y'(\boldsymbol{\rho}) \frac{\partial}{\partial \rho'} Y'(\boldsymbol{\rho}') \frac{1}{\rho'} \cdot \left[\frac{\rho - \rho' \cos \Delta\phi}{\rho^2 + \rho'^2 - 2\rho\rho' \cos \Delta\phi} \right]_{\rho = \varepsilon} dV' \, d\phi \right) \quad \text{(B11)}$$

where we use the notation $\Delta\phi = \phi - \phi'$. Finally

$$\lim_{t \to \infty} \frac{h_{b,\alpha}^{(2)}}{\ln t} = \frac{Q}{4\pi T_w} \cdot \left[\frac{(Y_w - \langle Y \rangle)^2}{2} - \frac{1}{4\pi^2} \lim_{\rho \to \infty} \rho \int_0^{2\pi} \int_0^{2\pi} \int_0^\rho Y'(\rho, \phi) Y'(\rho', \phi') \cdot \left(\frac{(\rho^2 + \rho'^2) \cos \Delta\phi - 2\rho\rho'}{(\rho^2 + \rho'^2 - 2\rho\rho' \cos \Delta\phi)^2} \right) d\rho' \, d\phi' \, d\phi \right] \quad \text{(B12)}$$

Now we go back to the remaining two terms in (B1), where we have the $\nabla_\rho^2 G$ term, given by (B2). With the same methodology as before, we can be prove that the part corresponding to the $\partial G / \partial t$ gives a zero contribution for large times. The part corresponding to the Dirac delta function, which we will call $h_{b,\gamma}^{(2)}$, can be rewritten as

$$h_{b,\gamma}^{(2)} = \int_V \frac{Q}{2\pi T_w} \frac{1}{\rho} Y'(\boldsymbol{\rho}) \frac{\partial}{\partial \rho} Y'(\boldsymbol{\rho}) \cdot \left[\int_0^t \exp\left(\frac{-\rho^2 S}{4T_G \tau}\right) G \, d\tau \right] dV - \int_V \frac{Q}{2\pi T_w} \frac{1}{\rho} Y'^2(\boldsymbol{\rho}) \cdot \left[\int_0^t \frac{1}{\tau} \exp\left(\frac{-\rho^2 S}{4T_G \tau}\right) G \, d\tau \right] dV \quad \text{(B13)}$$

which are again simple convolutions in time. Applying the same methodology, the second integral in (B13) gives a zero contribution of order $\ln t$, while the first integral leads to

$$h_{b,\gamma}^{(2)} = \int_0^{2\pi} \int_0^\infty \frac{Q}{2\pi T_w} \frac{1}{8\pi} \frac{\partial}{\partial \rho} Y'^2(\rho, \phi) \, d\rho\phi \quad \text{(B14)}$$

By direct integration, the final result is

$$\lim_{t \to \infty} \frac{h_{b,\gamma}^{(2)}(t)}{\ln t} = \frac{Q}{4\pi T_w} \left(\tfrac{1}{2} \overline{Y'^2}(R) - \tfrac{1}{2} 1 \, (Y_w - \langle Y \rangle)^2 \right) \quad \text{(B15)}$$

Acknowledgments. This work was funded by ENRESA (Spanish Nuclear Waste Management Company) and the EU. The authors appreciate the comments by H. Zhan and two anonymous reviewers.

References

Butler, J. J., Jr., Pumping tests in nonuniform aquifers—The radially symmetric case, *J. Hydrol.*, *101*, 15–30, 1988.

Butler, J. J., Jr., A stochastic analysis of pumping tests in laterally nonuniform media, *Water Resour. Res.*, *27*(9), 2401–2414, 1991.

Butler, J. J., Jr., and W. Z. Liu, Pumping tests in nonuniform aquifers: The radially asymmetric case, *Water Resour. Res.*, *29*(2), 259–269, 1993.

Carslaw, H. S., and J. C. Jaeger, *Conduction of Heat in Solids*, 510 pp., Oxford Sci. Publ., New York, 1959.

Cooper, H. H., Jr., and C. E. Jacob, A generalized graphical method for evaluating formation constants and summarizing well-field history, *Eos Trans. AGU*, *27*(4), 526–534, 1946.

Dagan, G., *Flow and Transport in Porous Formations*, 465 pp., Springer-Verlag, New York, 1989.

Desbarats, A. J., Spatial averaging of hydraulic conductivity in three-dimensional heterogeneous porous media, *Math. Geol.*, *24*(3), 249–267, 1992.

Durlofsky, L. J., Representation of grid block permeability in coarse scale models of randomly heterogeneous porous media, *Water Resour. Res.*, *28*(7), 1791–1800, 1992.

Erdélyi, A., W. Magnus, F. Oberhettinger, and F. G. Tricomi, *Tables of Integral Transforms*, vol. 1, 391 pp., McGraw-Hill, New York, 1954.

Gelhar, L. W., and C. L. Axness, Three-dimensional stochastic analysis of macrodispersion in aquifers, *Water Resour. Res.*, *19*(1), 161–180, 1983.

Gómez-Hernández, J. J., and S. M. Gorelick, Effective groundwater model parameter values: Influence of spatial variability of hydraulic conductivity, leakance, and recharge, *Water Resour. Res.*, *25*(3), 405–419, 1989.

Gómez-Hernández, J. J., and A. G. Journel, Joint sequential simulation of multiGaussian fields, in *Proceedings of the Fourth Geostatistics Congress*, vol. 1, pp. 85–94, Kluwer Acad., Norwell, Mass., 1993.

Herweijer, J. C., and S. C. Young, Use of detailed sedimentological information for the assessment of aquifer tests and tracer tests in a shallow fluvial aquifer, in *Proceedings of the 5th Annual Canadian/American Conference on Hydrogeology*, pp. 101–115, Natl. Water Well Assoc., Dublin, Ohio, 1991.

Hunt, B., Flow to a well in a multiaquifer system, *Water Resour. Res.*, *21*(11), 1637–1641, 1985.

Indelman, P., and B. Abramovich, A higher-order approximation to effective conductivity in media of anisotropic random structure, *Water Resour. Res.*, *30*(6), 1857–1864, 1994a.

Indelman, P., and B. Abramovich, Nonlocal properties of nonuniform averaged flows in heterogeneous media, *Water Resour. Res.*, *30*(12), 3385–3393, 1994b.

Indelman, P., A. Fiori, and G. Dagan, Steady flow toward wells in heterogeneous formations: Mean head and equivalent conductivity, *Water Resour. Res.*, *32*(7), 1975–1983, 1996.

Lachassagne, P., E. Ledoux, and G. de Marsily, Evaluation of hydrogeological parameters in heterogeneous porous media, in *Groundwater Management: Quantity and Quality*, *IAHS Publ. 188*, 3–18, 1989.

Matheron, G., *Elements Pour une Theorie des Milieux poreux*, 166 pp., Maisson et Cie, Paris, 1967.

Meier, P. M., J. Carrera, and X. Sánchez-Vila, An evaluation of Jacob's method for the interpretation of pumping tests in heterogeneous formations, *Water Resour. Res.*, *34*(5), 1011–1025, 1998.

Naff, R. L., Radial flow in heterogeneous porous media: An analysis of specific discharge, *Water Resour. Res.*, *27*(3), 307–316, 1991.

Neuman, S. P., and S. Orr, Prediction of steady state flow in nonuniform geologic media by conditional moments: Exact nonlocal formalism, effective conductivities, and weak approximation, *Water Resour. Res.*, *29*(2), 341–364, 1993.

Oliver, D. S., The averaging process in permeability estimation from well-test data, *SPE Form. Eval.*, *5*, 319–324, 1990.

Oliver, D. S., The influence of nonuniform transmissivity and storativity on drawdown, *Water Resour. Res.*, *29*(1), 169–178, 1993.

Sánchez-Vila, X., Radially convergent flow in heterogeneous porous media, *Water Resour. Res.*, *33*(7), 1633–1641, 1997.

Sánchez-Vila, X., I. Colominas, J. P. Girardi, and J. Carrera, *FAITH: User's Guide*, Univ. Politècn. de Catalunya, Barcelona, Spain, 1993.

Sánchez-Vila, X., J. Carrera, and J. P. Girardi, Scale effects in transmissivity, *J. Hydrol.*, *183*, 1–22, 1996.

Sánchez-Vila, X., C. L. Axness, and J. Carrera, Equivalent transmissivities in heterogeneous porous media under radially convergent flow, in *Proceedings of GeoENV, First European Conference for Geostatistics to the Environment*, pp. 1–12, Kluwer Acad., Norwell, Mass., 1997.

Schad, H., and G. Teutsch, Effects of the investigation scale on pumping test results in heterogeneous porous aquifers, *J. Hydrol.*, *159*, 61–77, 1994.

Serrano, S. E., The Theis solution in heterogeneous aquifers, *Ground Water*, *35*(3), 463–467, 1997.

Shvidler, M. I., *Filtration Flows in Heterogeneous Media (A Statistical Approach)*, Consult. Bur., New York, 1964.

Tiedeman, C. R., P. A. Hsieh, and S. B. Christian, Characterization of a high-transmissivity zone by well test analysis: Steady state case, *Water Resour. Res.*, *31*(1), 27–37, 1995.

J. Carrera, P. M. Meier, and X. Sánchez-Vila, Departament Enginyeria del Terreny i Cartogràfica, Universitat Politècnica de Catalunya, Gran Capita s/n, Modul D-2, 08034 Barcelona, Spain. (dsanchez@etseccpb.upc.es)

(Received January 29, 1998; revised December 31, 1998; accepted January 4, 1999.)